EARTH'S CRYOSPHERE
SCIENTIFIC JOURNAL

Earth's Cryosphere, 2022, vol. XXVI, No. 1, pp. 47–54 http://earthcryosphere.ru/

METHODS OF CRYOSPHERIC RESEARCH

GEORADAR STUDIES OF GROUND ICE IN THE COMPLEX OF ENGINEERING AND GEOLOGICAL SURVEYS

D.V. Kopylov[1,2], M.R. Sadurtdinov[2], S.Yu. Yanin[1]

[1] *Tyumen Petroleum Research Center, P.O.B. 747, Tyumen, 625000 Russia*
[2] *Earth Cryosphere Institute, Tyumen Scientific Centre Siberian Branch of the Russian Academy of Sciences, Malygina str. 86, Tyumen, 625026 Russia; kopylovdmitr@yandex.ru*

The results of ground-penetrating radar studies within the set of engineering and geological surveys at the site of designing a well pad in the oil and gas field in the area of continuous permafrost are considered. Drilling of geological wells with core sampling showed the presence of an ice-ground lens with the ice content of up to 90 %. Comparison of the drilling results and the characteristic wave pattern on georadar sections made it possible to identify the zone of anomalous changes in soil properties and interpret it as an ice-ground lens. High-amplitude diffractions of an electromagnetic wave are seen at the ice-ground/peat boundary, which, according to the authors, is associated with the presence of ice wedges. With the help of attribute analysis, the ice-ground lens has been was contoured and its approximate volume has been calculated.

Keywords: *attribute analysis, ground penetrating radar, geotechnical surveys, permafrost zone, ice-ground lens*

INTRODUCTION

The increasing development of oil and gas fields in the Arctic involves active construction of oil and gas infrastructure in the permafrost zone, where soils are in a changing field of negative or zero temperatures. Frozen rocks and ground ice are quite sensitive and unstable under anthropogenic impact, which leads to degradation or destruction of complex cryogenic systems. Therefore, information about the occurrence of thawing rocks with the high ice content is necessary in order to select the optimal and safe location for the foundations of structures, which is one of the main tasks of engineering geological surveys and geocryological studies.

Geotechnical surveys (GTS) in permafrost areas are carried out with the aim of a comprehensive assessment of modern engineering and geocryological conditions of the territory, including the geological structure; geomorphic and hydrogeological conditions; geocryological structure; composition, condition and properties of soils; and engineering and geological processes [*SP 11-105-97, 1999*]. In addition, within the framework of the GTS, a forecast is made of possible changes in engineering and geological conditions during the interaction of the designed objects with the geological environment.

In tundra areas with continuous permafrost, various types of cryogenic processes, both natural and technogenic, occur [*Alvanyan and Alvanyan, 2020*], which often do not have geomorphological features, especially in winter, when the snow cover smooths out all landforms. These processes, by their characteristic features, are not noticeable to a geologist during reconnaissance survey and route observation of the study area in the winter period of the year, and a large distance between reconnaissance boreholes often does not allow detecting areas of anomalous changes in permafrost properties. For example, according to [*SP 11-105-97, 1999*], the distance between engineering-geological boreholes along the pipelines in permafrost areas should be 100 m, whereas the size of polygonal ice wedges and talik zones in the plan can be the first meters. Geophysical methods implemented within the framework of a one-dimensional horizontally layered model of the environment, such as electrical and seismic sounding, which are performed with a step of 50–100 m or more, are also less informative in permafrost conditions. Reducing the step between sounding points is often cost-inefficient within the framework of GTS. In such cases, it is advisable to use geophysical surveys with noninvasive high-density observation systems. One of such methods of geophysics is georadiolocation (GRL) [*Ermakov and Starovoitov, 2010; Vladov and Sudakova, 2017*]. This paper discusses the results of the application of georadar studies in areas with a wide distribution of various morphological types of ground ice. The main purpose of the study was to detect and delineate ground ice within the area of the designed artificial structures, as well as to assess the possibility of using the wave field attribute (Q-factor) to identify ground ice bodies of various shapes.

EXPERIENCE IN GEORADAR RESEARCH WITHIN THE FRAMEWORK OF ENGINEERING AND GEOCRYOLOGICAL SURVEYS

Ground-penetrating radar (GPR) studies in engineering geological surveys are enshrined in the regulatory framework in the field of construction and housing and communal services of the Russian Federation with the entry into force of a new set of rules on engineering and geological surveys for construction in 2019 [*SP 446.1325800, 2019*]. According to this regulatory document, GPR refers to the main geophysical methods in solving problems of determining the location, depth, and shape of local inhomogeneities (ice, ice-rich rocks, and taliks) and studying geological processes. In addition, the development of domestic mass-produced equipment and software and popularization of the method at various conferences and seminars have greatly simplified the use of georadar research in engineering surveys.

In recent years, many papers have been published that highlight the experience of using the method in solving various problems in the area of permafrost distribution [*Bradford et al., 2005; Brosten et al., 2009; Hubbard et al., 2013; Sjoberg et al., 2015; Navarro et al., 2016; Campbell et al., 2018; Kopylov and Sadurtdinov, 2019; Sudakova et al., 2019; Wang and Shen, 2019; Ganiyu et al., 2020; Rey et al., 2020*]. Of domestic works, the thesis research [*Bricheva, 2018*] should be noted, which is completely devoted to the study of cryogenic objects using GPR. In it, the author presents the results of full-wave numerical simulation of cryogenic objects by the finite difference method in the time domain in the gprMax program. Wave patterns were obtained from bodies imitating in section a narrow triangular ice wedge, a wide triangular ice wedge, and a rectangular ice wedge. Synthetic radargrams show hyperbolic reflections from the edges of the wedges and horizontal reflections from the top and bottom of the rectangular wedge. The top of the wedges is distinguished by a high-amplitude horizontal in-phase axis. The paper presents the result of numerical simulation of a real ice wedge. A complex wave pattern with many pseudohyperbolic reflections is shown. Physical modeling was performed using a laboratory ground penetrating radar stand; a foam plastic model of the wedge was placed in sand and water. Owing to a high contrast of water and foam plastic, it was possible to identify the contours of the model wedge in the wave pattern. Modeling showed the possibility of isolating the top and bottom of the wedge depending on its shape and approximately estimating the geometry of the cryogenic body according to GPR data.

The paper [*Sokolov et al., 2020*] presents the results of mathematical and physical modeling of georadar measurements over ice bodies located in a frozen rock mass. During physical modeling, rectangular bodies specially made of river ice were placed in a box with frozen sand in the open air in the winter season at a negative temperature. Georadar profiling and sounding were carried out on the surface of the frozen rock. As a result of the experiment, the patterns of dynamic and kinematic characteristics of the electromagnetic signal at the boundaries of "frozen rock–ice–frozen rock" system were revealed. Criteria for identifying ice bodies in a frozen ground massif were obtained. Attention was focused on the fact that for the correct interpretation of the GPR data, it is necessary to have sufficiently complete a priori information about the geocryological structure of the studied frozen ground massif.

In these works, bodies of ice homogeneous in their internal structure were considered, which is very rare in nature. As a rule, wedges and lenses of ground ice contain interlayers of mineral soil, which contribute to the wave pattern of the georadar section during reflection and refraction of an electromagnetic wave in the course of georadar sounding, As a result, the GPR sections display a wave pattern that differs significantly from the model one.

The work of foreign colleagues [*Munroe et al., 2007*] presents the results of georadar studies in the area with polygonal ice wedges in northern Alaska. Areal works were carried out with a step of 50 cm between profiles in order to build a three-dimensional model of the medium. The SIR-3000 georadar with an antenna unit central frequency of 400 MHz was used. As a result of the analysis of slices of a three-dimensional model at a depth of 120 cm, high-amplitude extended anomalies were observed that characterized the polygonal network of ice wedges. The results of this study demonstrated the efficiency of GPR for detecting ground ice, provided that a high-density observation network is used with further construction of 3D models.

Among few scientific publications on georadar application within the framework of engineering and geological surveys in permafrost areas, the work presenting the results of georadar studies in the settlement of Lorino (Chukotka) is worth noting [*Tregubov et al., 2020*]. The degradation of permafrost under anthropogenic impacts was established for the territory of this settlement. A schematic map of dangerous cryogenic processes, such as thermokarst and thermal erosion, ice-rich permafrost, and soil heave was developed. The high efficiency of georadar survey in combination with engineering-geological data in assessing the dynamics of cryogenic processes was clearly shown.

With the development of the method, not only its hardware and methods of work but also software with procedures for processing and interpreting the initial data are being improved,. Often, the procedures for processing and interpreting GPR data follow from the currently well-developed method of seismic reflected waves [*Vladov and Sudakova, 2017*].

Thus, the work [*Wang et al., 2020*] demonstrates the results of georadar studies in permafrost area on the Tibetan Plateau. This e work was carried out in order to study the seasonally thawed layer (STL) and determine its thickness for the needs of human economic activity. As the STL had a heterogeneous composition with inclusions of pebbles and boulders, from which diffraction was observed on radargrams, it was difficult to unambiguously determine its thickness. To obtain a high-resolution wave pattern during processing, the method of reverse migration in the time domain (RTM) was applied to the radargrams, as a result of which the thickness of the STL and its structure were accurately determined. In recent decades, GPR data processing procedures based on the study of electrophysical properties have appeared. For example, in [*Denisov and Kapustin, 2010*], the authors propose a method of an automated backscattering field for processing and interpreting GPR data. The essence of the method lies in the search and detection of signals characterized by diffraction features formed as a result of the reflection of an electromagnetic wave from local objects. In automatic mode, points are analyzed on the GPR profile, the position of which coincides with the tops of diffraction reflections. The kinematic and dynamic characteristics of these diffraction reflections are attributes of the points under study. As a result of the analysis of the radargram, sections of attributes are built, calculated on the basis of both measured characteristics and correlation dependencies. One of the most significant attributes of the electromagnetic field analysis is the *Q*-factor (the ratio of the center frequency of the signal spectrum to its width) calculated by the formula:

$$Q = \frac{\omega}{\Delta\omega} = \frac{\omega}{2\delta},$$

where Q is the Q-factor; δ is the damping factor, and $\omega = 2\pi f$ is the circular frequency, Hz.

The meaning of the Q-factor lies in the fact that the higher its value, the less energy loss of an electromagnetic wave occurs when passing through the thickness of the soil and the slower this wave decays.

When an electromagnetic wave passes through pure ice without impurities, there are practically no reflections and refractions, and the attenuation of an electromagnetic wave is significantly lower than in soils with a low ice content [*Frolov, 1998; Yakupov, 2008; Neradovsky, 2013*]. The Q-factor attribute makes it possible to explore and map ice-rich rocks and ground ice using GPR.

STUDY AREA

The study area is located in the Tazovsky district of the Yamalo-Nenets Autonomous Okrug, within the Messoyakha Lowland confined to a negative neotectonic structure that experienced relative subsidence in the Late Quaternary. During its history, the terrace surface has been reworked as a result of thawing of massive ice, ice-wedges, and ice-rich permafrost. Geomorphologically, the study site belongs to the third marine terrace, composed of alluvial-marine deposits–sands, loams, and sandy loams, the thickness of which varies from 3 to 25 m. Holocene lacustrine-marsh deposits are ubiquitous and are confined to lake depressions with peatbogs of up to 6 m in thickness.

According to the scheme of the general geocryological zoning of the West Siberian Plate [*Geocryology of the USSR..., 1989*], the survey site is located in the northern zone of the Novy Urengoy subzone of the Messoyakha region. The high-latitude position of the region in a harsh climate predetermined the widespread, almost continuous development of permafrost, the thickness of which is 250–350 m and reaches 400–450 m in some cases. Taliks exist under large lakes and river beds. Permafrost in the study area has an epigenetic nature; the ice content of the upper horizons reaches 40–50 % and rapidly decreases with depth. In these deposits, strata consisting of layers of ice and icy loam are exposed.

In the study area, the leading factors influencing the formation of the temperature field are severe climatic conditions, snow accumulation and vegetation patterns, topography, composition of frozen rocks, and their ice content. The mean annual permafrost temperature is –5...–7 °C; in depressions with snow accumulation, it rises by 2–3 °C. Based on the results of temperature measurements in boreholes, the average temperature at a depth of zero annual temperature amplitudes (10 meters) was calculated equal to –3.0 °C (minimum –4.6 °C, maximum –1.8 °C). Permafrost in the survey area to a depth of drilling (12 m) is represented mainly by loamy sands; less often by loams and sands. Mineral deposits are covered from the surface with a moss-vegetation layer and peat. It should be noted that according to the authors [*Danilov, 1975; Vasil'chuk, 2018*] in the study area, paragenesis of ice wedges with bodies of massive ice can occur. One of the most common paragenetic combinations of ice is the coexistence of wedge and segregation ice in Holocene sediments overlain by peatlands and underlain by sandy-loamy soils. In addition, ice wedges from the peatland may penetrate below into underlying ice beds.

RESEARCH METHODOLOGY

A set of engineering-geological works was carried out in the study area, which included the collection, study, and systematization of survey and research materials of previous years; reconnaissance survey of the site; drilling of engineering-geological boreholes; geophysical and geocryological studies. Field work was performed in April. The drilling of engineering-geological boreholes was carried out by self-propelled

drilling rigs URB-2A2, using a core method "dry" at a minimum rotation speed, with a diameter of up to 160 mm, a depth of up to 12 m. If thawed soils were found, drilling was carried out with casing pipes to isolate the aquifer. In boreholes with permafrost, the temperature of the rocks was measured. Temperature observations were made in the boreholes with the ETC-0.1/10 set for field measurement of soil temperature with a TK 20/20 thermistor chain at depth intervals of 0.5 m to a depth of 5 m; then, to a depth of 10 m, with depth intervals of 1 m; and deeper, with depth intervals of 2 m; permafrost temperature at the bottom of boreholes was also measured.

Geophysical surveys were carried out using the GPR method on the projected sites using a grid of 50 × 50 m (Fig. 1*A*). An OKO-2 ground-penetrating radar (NPC "Geotech", Russia) with the antenna unit AB-150 of the dipole type was used. The GPR survey was performed in winter (Fig. 1*B*), when there was no seasonally thawed layer with increased electrical conductivity, which favorably affected the quality and depth of the measurements, because of the minimal attenuation of the electromagnetic wave in the upper part of the section. In addition, thin dense snow cover at the site smoothed out the uneven surface of the tundra, which improved georeferencing of the GPR data. The obtained data were processed using the Georadar-Expert software [*Denisov, 2021*]; time and depth sections were constructed, and an attribute analysis was performed using the *Q*-factor parameter [*Denisov and Kapustin, 2010*]. The electromagnetic wave velocity (*V*) was measured in the processing program from data on diffraction reflection on the radargram using a theoretical hyperbola. The dielectric permittivity (ε) was calculated using the formula:

$$\sqrt{\varepsilon} = \frac{V}{c},$$

where *V* is the propagation velocity of an electromagnetic wave, cm/ns; *c* is the speed of light in vacuum, cm/ns; ε is the permittivity, c.u.

Fig. 1. Scheme of GPR survey (*A*) and general view of the site in winter (*B*) and summer (*C*).

(*1*) GPR profile and its number, (*2*) profile direction, and (*3*) engineering-geological borehole and its number.

RESULTS AND DISCUSSION

For design of infrastructure facilities, the upper part of the section of Quaternary deposits serving as the basis for the designed objects is of major interest. Frost cracking and ice wedge formation associated with it are developed in the study area. The survey site is surrounded by numerous shallow (0.4–0.6 m) thermokarst lakes, both saucer-shaped and elongated.

The geological structure of the study area (Fig. 2) down to a depth of 12 m includes the following lithogenetic complexes: Late Quaternary marine and alluvial sediments of the third sea terrace and Holocene biogenic deposits. The moss-vegetation and uppermost soil layers are exposed at depths from 0 to 0.2 m, their thickness varies from 0.1 to 0.2 m. Below, Holocene biogenic deposits represented by frozen low-ice peat with a layered cryostructure. are found at depths of 0.4 to 6.1 m. A characteristic feature of the engineering-geological section at the study site is the presence of ice-bonded mineral layers in the peat and at its lower boundary. The ice content is such layers may reach 90 % and more. These layers occur at depths of 0.4–4.7 m, and their bulk density reaches 0.83 g/cm^3. Their maximum thickness is 3.7 m. Thermometric observations in the borehole with such ice-bonded mineral layers on April 16, 2018 indicated the minimum temperature of –12.2 °C at a depth of 1.4 m.

Figure 3 shows the time (Fig. 3*a*) and deep (Fig. 3*b*) georadar sections along profile No. 6, passing

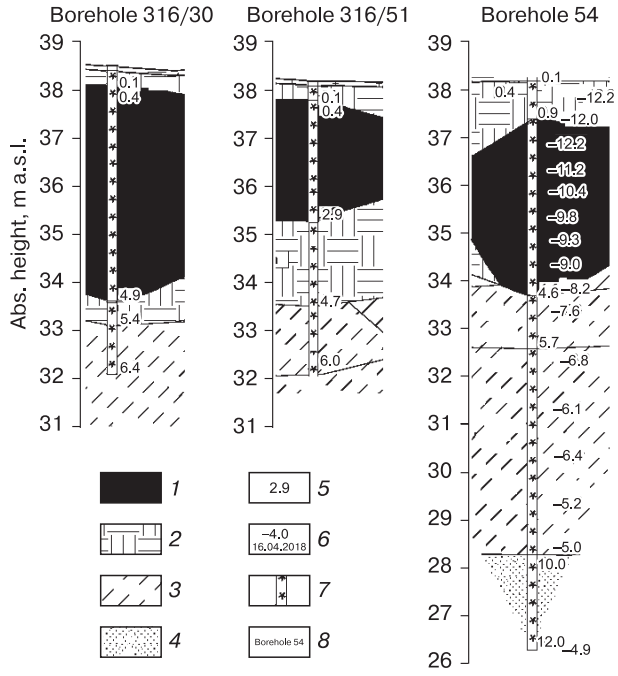

Fig. 2. Geological sections according to drilling data.

(*1*) ice-rich mineral ground; (*2*) low-ice frozen peat; (3) well-bonded low-ice loamy sand; (*4*) well-bonded low-ice sand, (*5*) depth of the base of the layer, m; (*6*) ground temperature (°C) and date of its measurement; (*7*) designation of the state of the soil (frozen soil); and (*8*) borehole number.

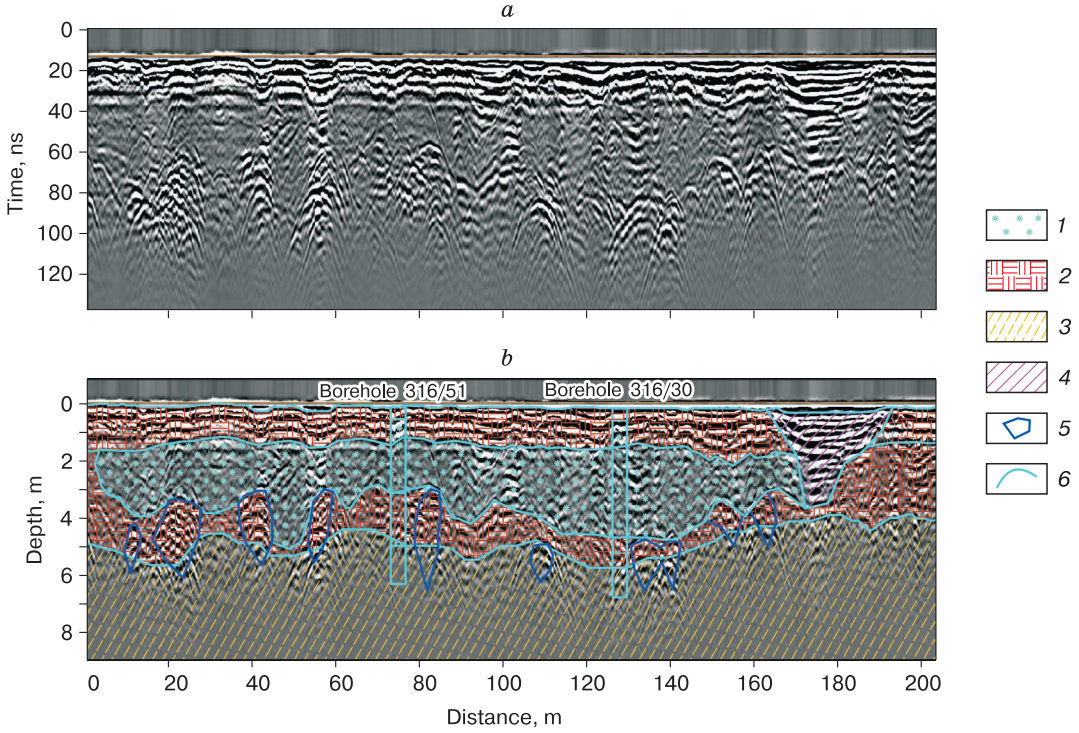

Fig. 3. Temporal (*a*) and depth (*b*) georadar sections along profile 6:

(*1*) ice-rich mineral ground, (*2*) frozen peat, (*3*) frozen loamy sand, (*4*) thawed loam, (*5*) presumed ice bodies, and (*6*) lower boundary of GPR signal.

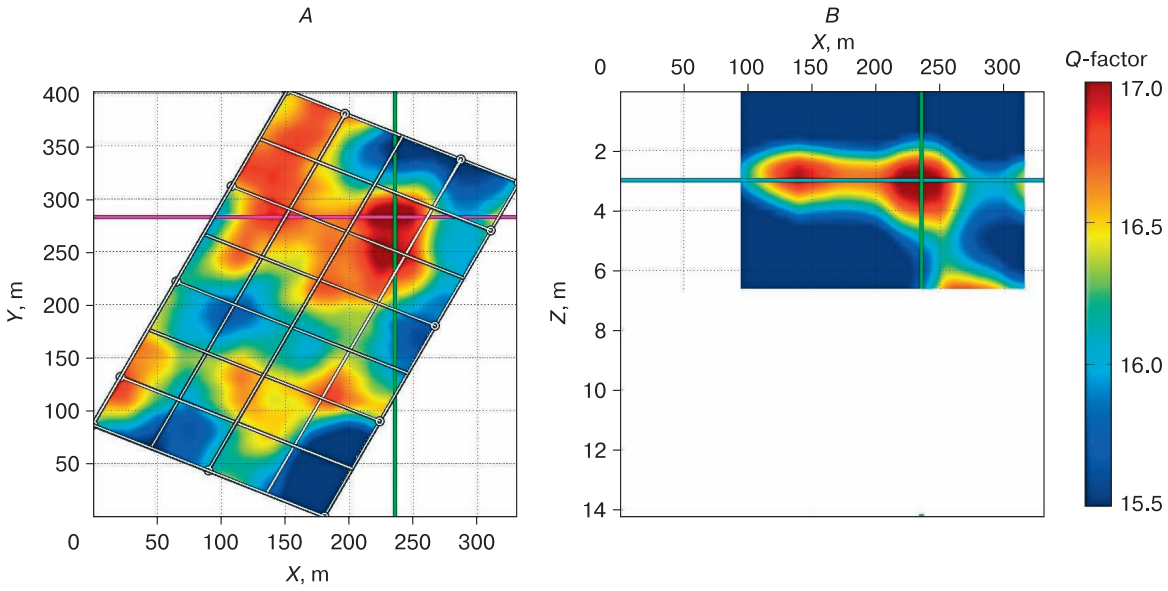

Fig. 4. Sections of the pseudo-3D model according to the *Q*-factor attribute:

(*A*) *X*–*Y* section at a depth of 3 m, (*B*) *X*–*Z* section, and (*C*) *Y*–*Z* section.

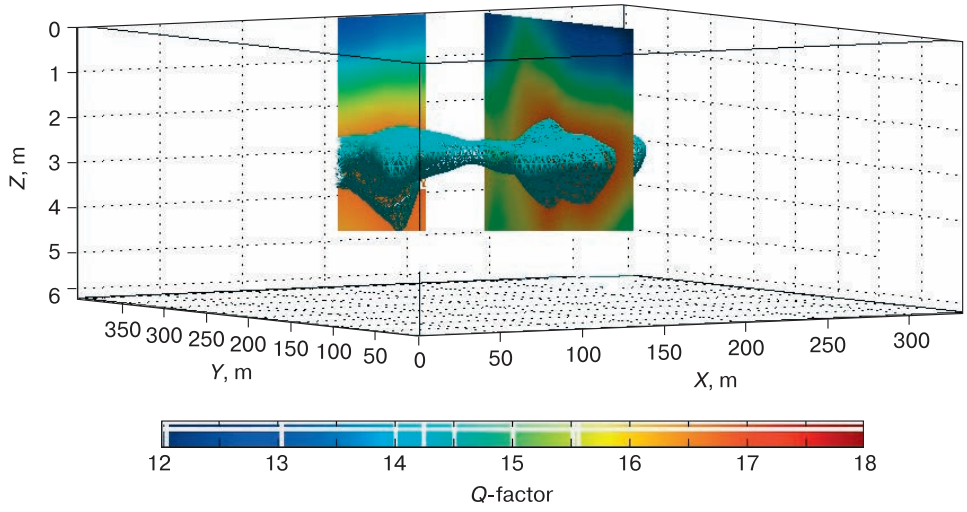

Fig. 5. Volumetric pseudo-3D model of the ice-ground lens.

through the ice bonded ground lens penetrated by boreholes Nos. 316/30 and 316/51.

On the georadar section (Fig. 3*b*), layers with different dielectric constants are distinguished along the common-mode axes. The section is complicated by the lateral variability of soils and the presence of anomalous bodies. The first GPR layer from the surface with parameters V = 13.0 cm/ns, ε = 5.0 and thickness of up to 2 m is distinguished by high-amplitude common-mode axes. This layer includes the snow cover from the top and the frozen low-ice peat under it. Differences in the thickness of the layers as measured in boreholes and according to GPR data are due to some distance (up to 15 m) of the boreholes from the GPR profile. In the interval of 5–170 m along the GPR profile, an anomalous zone is distinguished from a depth of 1.8 m and having a thickness of up to 3.0 m; in this zone, V = 16.6 cm/ns, and ε = 3.2. It corresponds to ice-rich mineral layer. Chaotic reflections in the body of this layer attest to the presence of soil impurities in the ice, from which the electromagnetic wave is reflected. A very unusual picture is observed at the lower boundary of the ice-rich layer at the contact with peat: there are many high-amplitude diffractions of an electromagnetic wave. Permittivity values in this zone (ε = 2.9–3.4) correspond to ice. According to [*Bricheva, 2018*], numerical modeling of ice wedges of various shapes attests to the presence of diffraction hyperbolas from the wedges and their edges. In other study in the area with analogous climatic and geological conditions [*Tregubov et al., 2019*], diffraction reflections from local ice bodies were also observed. Based on the foregoing, the authors associate the presence of diffraction reflections of an electromagnetic wave at the base of the ice-rich mineral layer with the occurrence of ice wedges.

It should be noted that the distance between neighboring georadar profiles (50 m) did not allow to outline the network of ice wedges in plane. To do this, georadar profiles should be spaced apart at smaller distances. To confirm the presence of ice wedges at the base of the ice-rich mineral lens, verification by drilling in places of concentration of diffracted reflections is required.

Using attribute analysis, sections of the pseudo-3D model were obtained from the Q-factor attribute (Fig. 4), which made it possible to display the spatial distribution of the ice-ground lens. Local ice wedges are not distinguished by the Q-factor attribute. This is explained by the fact that the electromagnetic wave is reflected and refracted from the local bodies of ice wedges quite intensively, so that it loses its energy and decays. As the value of the Q-factor attribute is inversely proportional to the attenuation of the electromagnetic wave, local ice wedges cannot be distinguished from the host rocks on the radargrams by the Q-factor attribute.

As a result of georadar survey, the pseudo-3D model of the surveyed area was built (Fig. 5). Based on the isosurface of the 3D model, the volume of the underlying ice-ground lens was estimated at approximately 20 795 m^3.

CONCLUSIONS

As a result of the research, an ice-rich mineral lens has been detected within the layer of low-ice peat. On radargrams, this lens appeared as an anomalous zone with the absence of in-phase axes, which indicates a low attenuation coefficient of the electromagnetic wave amplitude. High-amplitude diffraction reflections at the lower boundary of the ice-rich mineral lens with the underlying peat are probably associated with the presence of ice wedges. Attribute analysis of georadar data with the use of the Q-factor parameter makes it possible to identify the ice-rich mineral lens, whereas local ice wedges cannot be distinguished. Based on the isosurface of a three-dimensional pseudo-3D model, the volume of the ice-rich mineral lens has been calculated. For a more accurate quantitative analysis of georadar data, it is necessary to reduce the distance between neighboring georadar profiles to 0.5–1 m. According to the authors, the presence of various forms of electromagnetic wave reflections on the wave patterns, which are characteristic of the ice–ground lens and of the bodies of ice wedges, indicate their paragenesis, which is very common in the study area. To confirm this, it is necessary to verify anomalous areas on radargrams by drilling method.

References

Alvanyan, A.K., Alvanyan, K.A., 2020. Geocryology: A Textbook. Perm State National Research University, Perm, 139 p. (in Russian).

Bradford, J.H., McNamara, J.P., Bowden, W., Goose, M.N., 2005. Measuring thaw depth beneath peat-lined arctic streams using ground-penetrating radar. Hydrol. Proc. **19** (14), 2689–2699.

Bricheva, S.S., 2018. Development of a method for studying cryogenic objects using ground-penetrating radar. Cand. Sci. (Geol. Mineralog.) Dissertation. Moscow, 169 p. (in Russian).

Brosten, T.R., Bradford, J.H., McNamara, J.P. et al., 2009. Estimating 3D variation in active-layer thickness beneath arctic streams using ground-penetrating radar. J. Hydrol. **373**, 479–486.

Campbell, S., Affleck, R.T., Sinclair, S., 2018. Ground-penetrating radar studies of permafrost, periglacial, and near-surface geology at McMurdo Station, Antarctica. Cold Reg. Sci. Technol. **148** (4), 38–49.

Danilov, I.D., 1975. Ice formation in Formation ice in subaqual deposits of the north of Western Siberia. Prirodn, Uslov. Zap. Sibiri, No. 5, 205–215 (in Russian).

Denisov, R.R., 2021. Software package for automated processing of geo-radar data. Georadar-Expert. Manual. URL: http://www.georadar-expert.ru/download/georadar/expert/manual/rus.pdf (last visited: November 15, 2021).

Denisov, R.R., Kapustin, V.V., 2010. Processing of GPR data in automatic mode. Geofizika, No. 4, 76–80 (in Russian).

Ermakov, A.P., Starovoitov, A.V., 2010. The use of the ground penetrating radar (GPR) method in engineering-geological studies for the assessment of geological-cryological conditions. Moscow Univ. Geol. Bull. **65** (6), 422–427.

Frolov, A.D., 1998. Electrical and elastic properties of frozen rocks and ice. Pushchino, ONTI PNTs RAN, Pushchino, 515 p. (in Russian).

Ganiyu, S., Oladunjoye, M., Onakoya, O. et al., 2020. Combined electrical resistivity imaging and ground penetrating radar study for detection of buried utilities in Federal University of Agriculture, Abeokuta, Nigeria. Environ. Earth Sci. **79** (8), doi: 10.1007/s12665-020-08919-2

Geocryology of the USSR. Western Siberia, 1989. Nedra, Moscow, 454 p. (in Russian).

Hubbard, S., Gangodagamage, C., Dafflon, B. et al., 2013. Quantifying and relating land-surface and subsurface variability in permafrost environments using LiDAR and surface geophysical datasets. Hydrogeol. J. **21** (1), 149–169.

Kopylov, D.V., Sadurtdinov, M.R., 2019. Using geoelectrical prospecting for engineering-geocryological studies on objects of oil and gas infrastructure. Ekspozitsiya Neft'–Gaz, No. 6 (73), 12–15 (in Russian).

Munroe, J.S., Doolittle, J.A., Kanevskiy, M.Z. et al., 2007. Application of ground-penetrating radar imagery for three-dimensional visualisation of near-surface structures in ice-rich permafrost, Barrow, Alaska. Perm. Perigl. Proc. **18** (4), 309–321, doi: 10.1002/ppp.594

Navarro, F., Lapazaran, J., Martin-Espanol, A., Otero, J., 2016. Ground-penetrating radar studies in Svalbard aimed to the calculation of the ice volume of its glaciers. Cuad. Investig. Geograf. **42** (2), doi: 10.18172/cig.2929

Neradovsky, L.G., 2013. Experience of using georadiolocation in the northeast North-East of Yakutia. Inzhenern. Izyskan., No. 2, 26–37 (in Russian).

Rey, J., Martinez, J., Hidalgo, M. et al., 2020. Ground penetrating radar study of progradational units in Holocene coastal plains: Carchuna Beach (SE Spain). Geosciences **10** (7), 277.

Sjoberg, Y., Marklund, P., Pettersson, R., Lyon, S.W., 2015. Geophysical mapping of palsa peatland permafrost. The Cryosphere **9** (2), 465–478.

Sokolov, K.O., Fedorova, L.L., Fedorov, M.P., 2020. Prospecting and evaluation of underground massive ice by ground-penetrating radar. Geosciences **10** (77), 274.

SP 11-105-97, 1999. Engineering geological surveys for construction. Part IV. Rules and regulations on geophysical surveys. Gosstroi RF, Moscow, 58 p. (in Russian).

SP 446.1325800, 2019. Engineering and geological surveys for construction. General rules for the production of works. Standartinform, Moscow, 80 p. (in Russian).

Sudakova, M.S., Sadurtdinov, M.R., Carev, A.M. et al., 2019. GPR capabilities for studying wetlands in the permafrost zone. Geol. Geofizika **60** (7) 1004–1013 (in Russian).

Tregubov, O.D., Kraev, G.N., Maslakov, A.A., 2020. Hazards of activation of cryogenic processes in the Arctic Community: a geopenetrating radar study in Lorino, Chukotka, Russia. Geosciences **10** (2), 57.

Tregubov, O.D., Nuteveket, N.A., Uyagansky, K.K., 2019. The application of ground penetrating radar (GPR) at the interpretation of engineering survey data of the past years: massive ice beds or ice wedges? In: Conf. Proc. Engineering and Mining Geophysics: 15th Conference and Exhibition, April 2019, vol. 2019, p. 1–10.

Vasil'chuk, Yu.K., 2018. Paragenetic ensembles of wedge ice with ice of different geneses. Arktika Antarktika, No. 2, 71–112 (in Russian).

Vladov, M.L., Sudakova, M.S., 2017. Ground-Penetrating Radar. From the Physical Basics to Promising Areas. Training Manual. GEOS Publ. House, Moscow, 240 p. (in Russian).

Wang, Q., Shen, Y., 2019. Calculation and interpretation of ground penetrating radar for temperature and relative water content of seasonal permafrost in Qinghai-Tibet Plateau. Electronics **8** (7), 731.

Wang, Y., Fu, Z., Lu, X., Qin, S. et al., 2020. Imaging of the internal structure of permafrost in the Tibetan Plateau using ground penetrating radar. Electronics **9** (1), 56–70.

Yakupov, V.S., 2008. Geophysics of Permafrost Areas. Yakutsk. Univ. Press, Yakutsk, 342 p. (in Russian).

Received August 16, 2021
Revised January 13, 2022
Accepted January 19, 2022

Translated by A.V. Muravyov